Proceedings of the
4th JSME-KSME Thermal Engineering Conference
October 1-6, 2000, Kobe, Japan

SYNTHESIZED MIXING PROCESS IN AN ACTIVELY-CONTROLLED CONFINED COAXIAL JET

Yuji SUZUKI*, Nobuhide KASAGI, Yasuhiro HORIUCHI, and Daiki NAGOYA
Department of Mechanical Engineering, The University of Tokyo
Hongo, Bunkyo-ku, Tokyo 113-8656

A novel coaxial jet nozzle equipped with a row of miniature electromagnetic flap actuators on its outer lip of the annular nozzle is developed for active mixing control. The spatio-temporal flow structures of the controlled jet discharging into an expanded circular duct are studied through flow visualization and quantitative measurements by using laser Doppler velocimetry and laser induced fluorescence. It is found that the large scale vortical structures emerging from the shear layer between the annular jet and the ambient fluid is significantly strengthened with the artificial disturbances generated by the flaps. The mixing between the inner and outer jets are markedly enhanced through the vigorous pinching of the central fluid.

Keywords: Coaxial Jets, Mixing Control, Electromagnetic Flap Actuators, LIF

1. INTRODUCTION

With growing attention to the environmental issues, reduction of NOx emission has become a very important design target for various kinds of combustors. Since the amount of thermal NOx depends primarily on high temperature spots in a flame, the lean premixed combustion mode is often employed in order to control the temperature field in a combustor chamber. However, since premixed combustion is only stable in a relatively narrow fuel-to-air ratio range, sophisticated design is required for suppressing blowout and/or oscillation combustion.

In gas-fueled combustors such as those in gas turbines, coaxial jets are often employed, in which two coannular fluid streams of fuel and air at different speed are discharged into a sudden expansion. In order to maintain stable combustion, a swirler and/or a flame holder using a bluff body are usually employed. However, these devices introduce large pressure drop through the nozzle, and it is generally difficult to keep adequate combustion condition for various operation condition. Therefore, a more advanced flow management method is desired especially for so-called micro gas turbines used for the distributed energy system, which are exposed to large load fluctuations.

Recently, active control of turbulent shear flows attracts much attention [1-3]. Since the large-scale coherent structures emerging in various shear flows play a dominant role in the turbulent heat and momentum transport [4-6], selective manipulation of these structures is desired in order to obtain efficient control effect. Recent development of MEMS (Microelectro-mechanical Systems) technology enables us to fabricate micro actuators, which are small enough to impose direct control input on the coherent structures [7, 8]. Liu et al.[9] showed that the rolling moment of a delta wing is efficiently controlled by micro magnetic flap actuators placed on the leading edge. Smith and Glezer[10] fabricated miniature zero-mass-flux jet actuators. They showed that a macro-scale planar jet can be vectored due to the formation of low-pressure recirculating flow regions near the flow boundary. Huang et al.[11] developed an on-chip electrostatic actuator integrated with a pressure sensor to detect and control screech in a high-speed air jet. Suzuki et al. [12] developed a novel axisymmetric nozzle, equipped with a row of miniature flap actuators on its nozzle lip, and investigated the response of the jet flow to various control modes. They found that the entrainment rate of the jet is significantly increased when furcating jet is generated by adding disturbances locally into the jet shear layer.

The final goal of the present study is to develop a new design strategy for low-NOx coaxial jet combustors with the active mixing control of fuel and air. As the first step, the control scheme developed by Suzuki et al.[12] is extended to mixing enhancement of an isothermal confined coaxial jet. The flap actuators are mounted on the periphery of the outer annular nozzle exit in order to manipulate vortex structures in the shear layer between the annular jet and the ambient still fluid. The response of the coherent structures to various control modes are examined by using flow visualization, and

quantitative measurement of velocity and concentration fields.

2. EXPERIMENTAL SETUP

A schematic of the flow configuration is shown in Fig. 1. A coaxial jet of water was issued into an expanded circular tube having 80 mm in diameter. The central jet flow was supplied from a long straight tube (diameter, D_i=10 mm), in which a fully-developed laminar flow was established. The annular flow was discharged through a 42:1 area ratio nozzle with an exit diameter of D_o=20mm. By considering the operation condition of lean premixed combustors, measurements were made at a large velocity ratio of 5. The bulk mean velocities of the central and annular parts of the nozzle are respectively set to be $U_{m,i}$=20 mm/s and $U_{m,o}$=100 mm/s, which are equivalent to the Reynolds numbers of 200 and 2000.

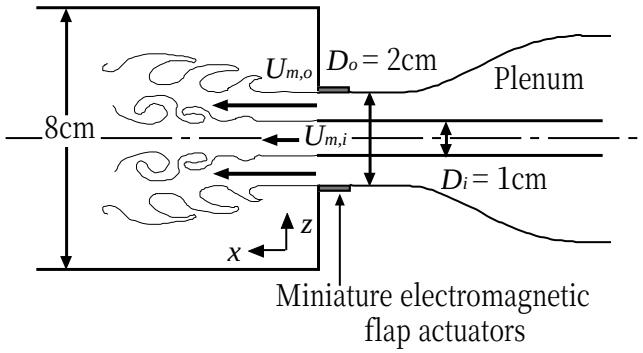

Figure 1 Confined coaxial jet.

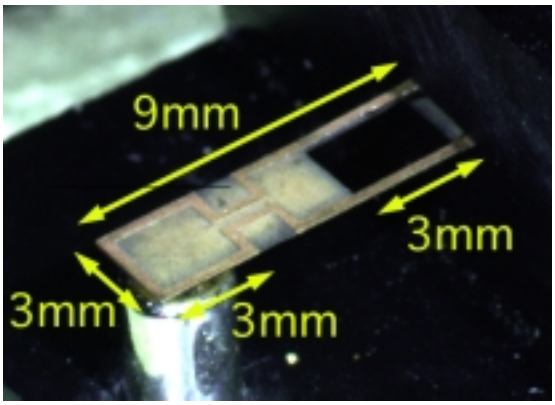

Figure 2 Electromagnetic flap actuator [12].

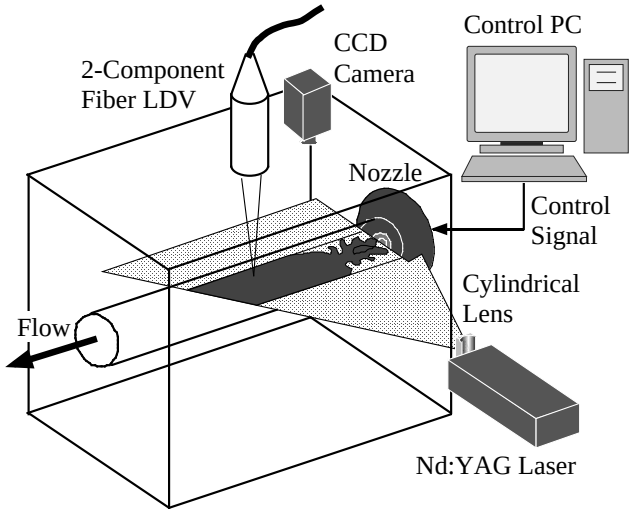

Figure 3 Experimental Setup.

Au & Ko [13] and Rehab et al. [14] separately showed that the outer jet dominates the near-field flow structure when the velocity ratio of coaxial jets is large. Therefore, actuators are placed inside the nozzle exit of the annular nozzle as shown in Fig. 1. The Cartesian coordinate system is employed, where x denotes the streamwise direction, while y and z are respectively the two perpendicular (vertical and horizontal) radial directions.

Figure 2 shows an electromagnetic flap actuator developed by Suzuki et al. [12]. The flap is made of a copper plated polyimide film having 9 mm in length and 3 mm in width. Film thickness is respectively 25 μm and 35 μm for the polyimide and copper layer. When an electric current is applied to the copper coil, the flap is elastically bent by the electromagnetic force between the coil and a cylindrical permanent magnet placed underneath. At the root of the flap, a part of the polyimide film is hollowed with a laser machining system to reduce the bending stiffness. In total, 18 electromagnetic flap actuators were placed inside the nozzle exit at a regular interval and covered 86% of the circumference. Each flap is driven independently by a control signal from a multichannel digital-analog board. The maximum displacement of the flap was set to be about 0.4 mm. The flap actuator employed in the present study could not survive high temperature circumstances in combustion chamber, but we concentrate on evaluating the active control scheme with an actuator currently available.

Figure 3 shows the arrangement of the measurement system. The expanded tube is made of Plexiglas and submerged into a water tank to eliminate light refraction at the tube wall. In order to examine the global behavior of large-scale structures and the entrainment/mixing characteristics qualitatively, the jet flow was visualized by using fluorescent dye (Rhodamine B; 0.5 ppm). The dye is injected into the bulk fluid of the inner jet as well as the outer shear layer from an annular slit inside the outer nozzle. A laser sheet from a 25 mJ Nd:YAG pulsed laser (Newwave Research; Mini/Lase PIV) is employed for illumination. The visualized images are acquired by a progressive scan CCD camera (Sony; XC-7500) and a frame grabber (Matrox, Meteor II/MC) at 60 frames per second. Velocity measurements are made with a two-component fiber LDV (Dantec; 60X11) with a 4W Ar ion laser. At each measurement station, statistics and power spectra are computed from more than 15000 velocity samples at a sampling frequency on the order of 100 Hz.

3. RESULTS

3.1 Flow visualization

A typical longitudinal sectional view of a natural jet is shown in Fig. 4(a). The laser light sheet cuts through the jet axis. A laminar shear layer separates from the outer nozzle lip and roles up into vortex rings at around $x/D_o = 2$. These vortices pinch off the inner jet and break down into turbulence at $x/D_o \sim 3$. The mixing between the central and annular fluids is fairly small near the nozzle exit, and the dye concentration along the jet centerline is almost constant at $x/D_o < 1$. Thus, the length of the inner potential core is about 1 D_o, which is in agreement with the previous result at a higher Reynolds number [13]. Au & Ko [13] also found that the Strauhal number St (= $f_p D_o/U_o$) corresponding to the natural pinching-off frequency f_p is 0.4. In the present study, however, St is 1.2, which is much larger than the previous result.

The vortex structures are dramatically changed by the action of the actuators. Figure 4(b) shows a longitudinal sectional view of the jet controlled by axisymmetric flap motion (Coaxial Mode, hereafter), in which all 18 flaps are driven in phase by a square wave signal of f_a = 6 Hz ($St_a = f_a D_o/U_o$ = 1.2). Strong axisymmetric vortex rings are shed with a regular spacing, which are synchronized with the flap motion. These vortices pinch off the inner fluid close to the nozzle exit vigorously, and thus the mixing is significantly enhanced. The dye concentration is rapidly decreased along the jet axis, so that the length of the potential core should be decreased. Although it is not shown here, flow visualization at various flapping frequencies indicates that the length of the potential core becomes minimum when $f_a \sim 6$ Hz. Therefore, periodic disturbances close to the natural pinching-off frequency should be effective for Coaxial Mode.

Suzuki et al. [12] found in their free jet experiment that when each half cluster of flaps are driven out of phase (Alternative Mode, hereafter), the jet clearly bifurcates into two branches and the entrainment is significantly enhanced. They also showed that the optimum flapping Strauhal number is the subharmonic of the preferred mode. Figure 4(c) shows a longitudinal sectional view presently obtained for Alternative Mode at f_a = 3 Hz (St_a = 0.6). An asymmetric vortex, which is much larger than that for Coaxial Mode, is observed near the nozzle exit, and the jet bifurcates into two separate branches from $x/D_o = 2$. Flow visualization result shown in Fig. 4(d) confirms that the vortex structure is symmetric in the bisecting plane.

Figures 5 and 6 respectively show successive flow visualization images for Coaxial Mode (St_a = 1.2) and Alternative Mode (St_a = 0.6). Unlike in the natural jet, strong vortices roll up close to the nozzle in both controlled modes. The pinching of the inner jet starts at $x/D_o \sim 0.25$, and the length of the inner potential core is significantly reduced.

In Alternative Mode, two vortices are shed during one cycle of the flap movement as in the bifurcating free jet [12]; one half vortex is generated by the flap ascending toward the jet centerline, while the other half is generated by the flap descending toward the nozzle inside wall. As the vortices convected, they are transported away from the center line. These asymmetric

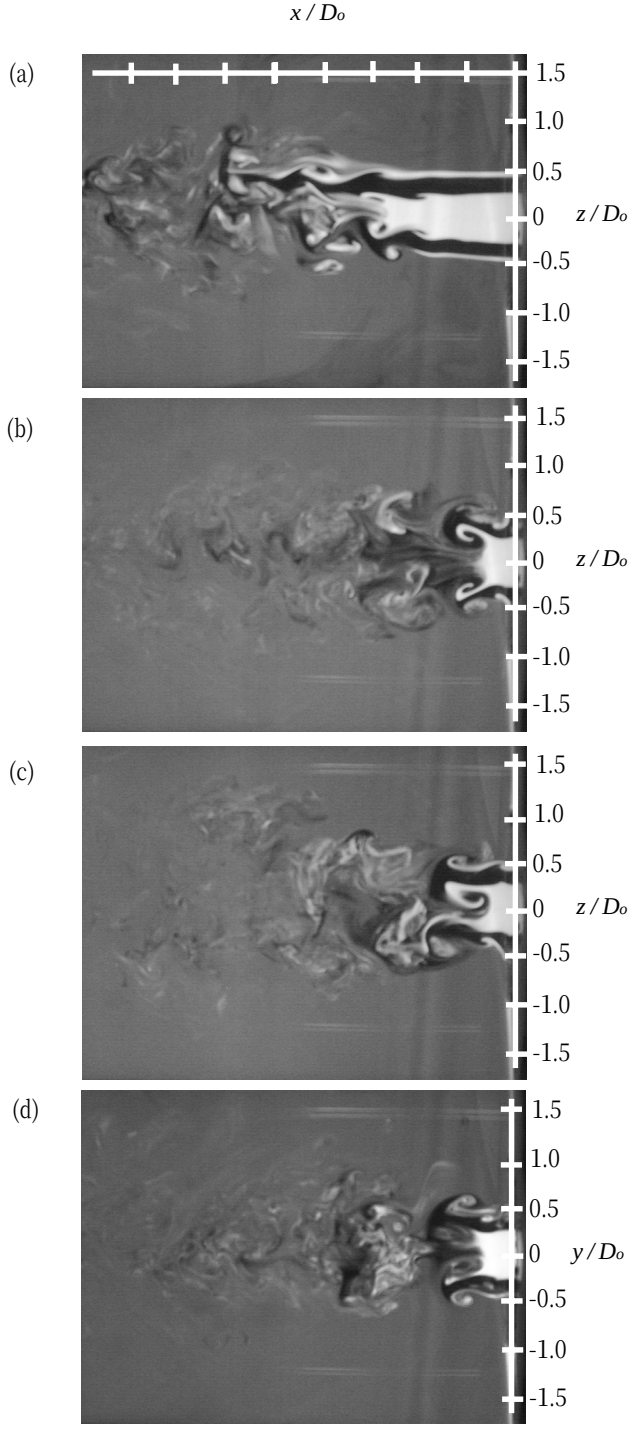

Figure 4 Longitudinal sectional view of the natural and controlled jets; (a)Natural jet, (b)Coaxial Mode (6Hz), (c)Alternative Mode in the bifurcating plane (3Hz), (d)Alternative Mode in the bisecting plane (3Hz).

vortices are much larger than those in Coaxial Mode, and they carry larger amount of fluid out of the inner jet. It is also indicated that the length of the inner potential core is somewhat smaller than that for Coaxial Mode.

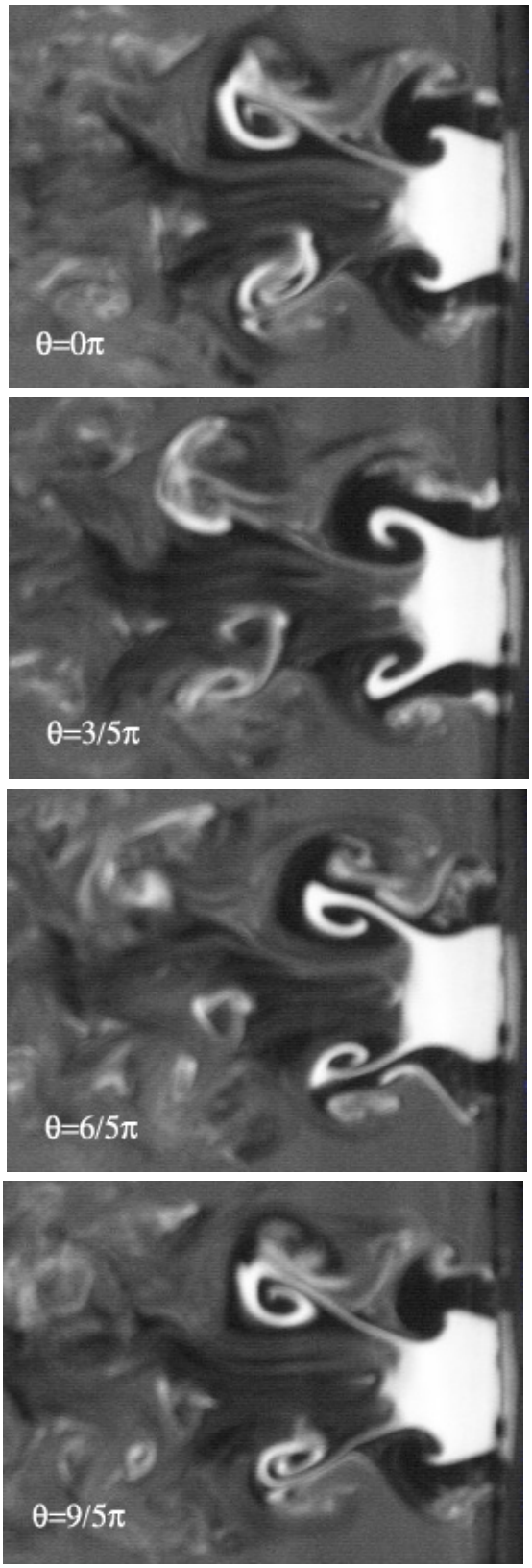

Figure 5 Successive flow visualization images near the nozzle exit for Coaxial Mode at f_a=6Hz.

3.2 Velocity measurement

Figure 7(a) shows the streamwise mean velocity U along the jet axis for Coaxial Mode at various flapping frequencies. In the natural jet, U is slightly decreased close to the nozzle exit, followed by a rapid increase due to the inrush of the outer vortex structures, and has

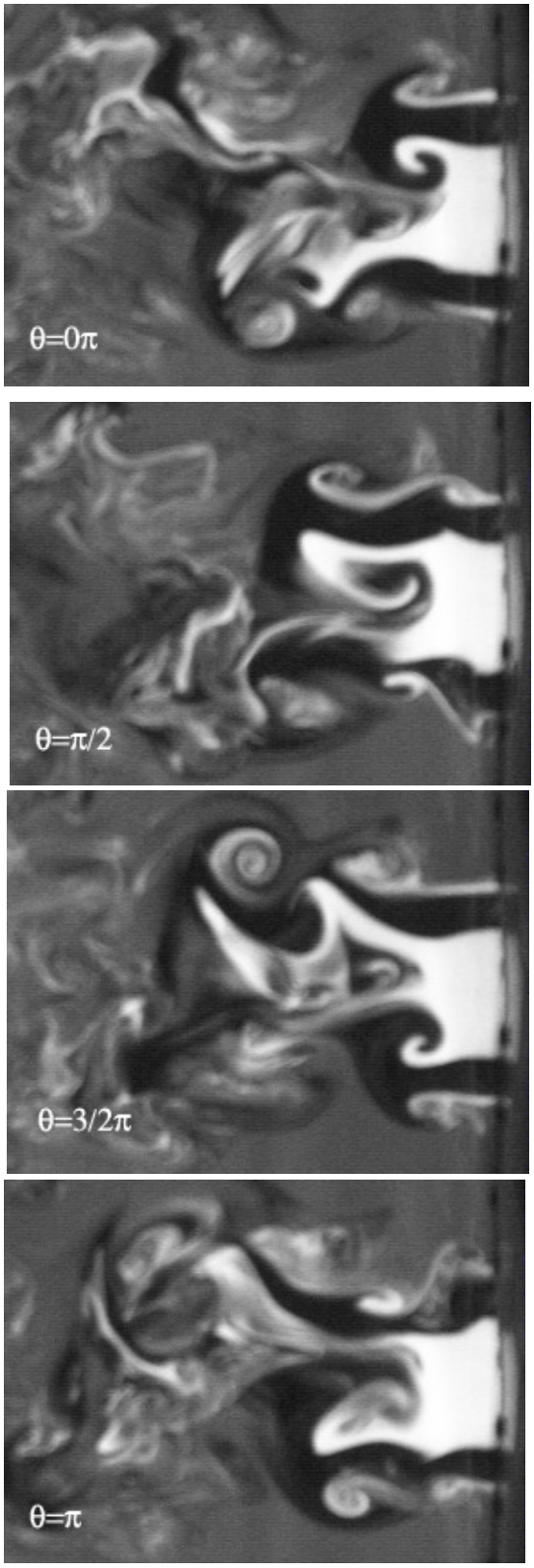

Figure 6 Successive flow visualization images near the nozzle exit for Alternative Mode at f_a=3Hz.

a peak at around x/D_o = 3. For controlled jets, U close to the nozzle exit is reduced. On the other hand, at x/D_o > 0.5, U is rapidly increased, and the peak is shifted closer to the nozzle exit. These facts are in accordance with the flow visualization results shown in Fig. 5. For Alternative Mode, U at x/D_o = 0.5 becomes negative as shown in Fig. 7(b). Thus, recirculation should be dominant in this region.

The flow reversal rate at x/D_o = 0.5 is shown in Fig. 8. For the natural jet, recirculation is not observed. Rehab et al. [14] show that the unsteady recirculation bubble is generated only if the velocity ratio is larger than a critical value of 8. Since the velocity ratio of the present study is 5, so that the present result is in accordance with their finding. On the other hand, the flow reversal rate is very large for the controlled jets when the flapping frequency is 3 - 6 Hz. It is conjectured that the larger flow reversal rate for Alternative Mode is due to the larger magnitude of the vortices near the nozzle exit.

(a)

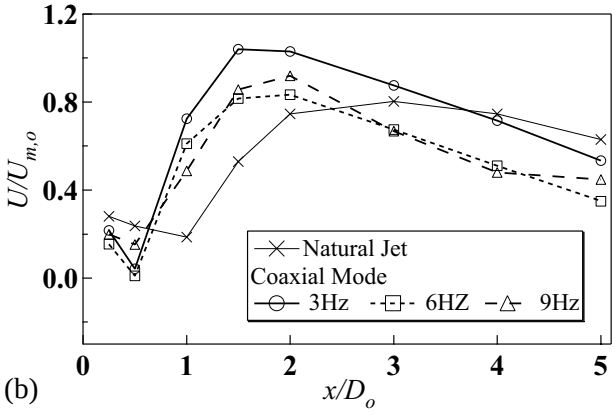

(b)

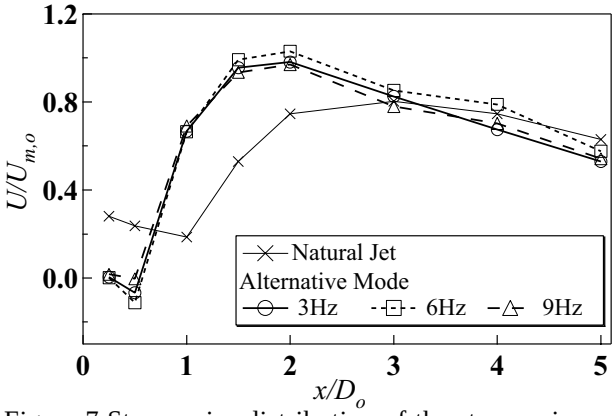

Figure 7 Streamwise distribution of the streamwise mean velocity along the jet axis; (a) Coaxial Mode (6Hz), (b) Alternative Mode (3Hz).

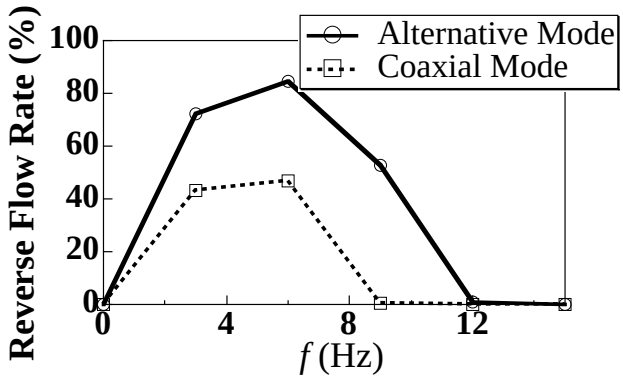

Figure 8 Reverse flow rate at x/Do=0.5.

3.3 Scalar measurement

In order to evaluate the mixing characteristic for the controlled jets, concentration field was measured by using a planar laser induced fluorescence (PLIF). The inner jet was seeded with the fluorescent dye, while pure water was supplied to the annular jet fluid. In total, 1800 image samples were employed to obtain ensemble-averaged statistics. Figures 9 (a) - (c) show the radial

(a)

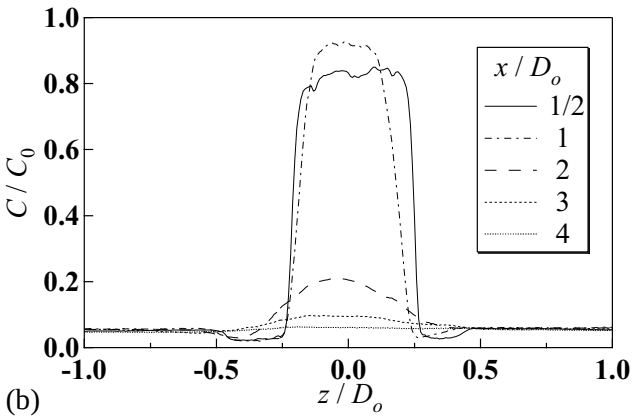

(b)

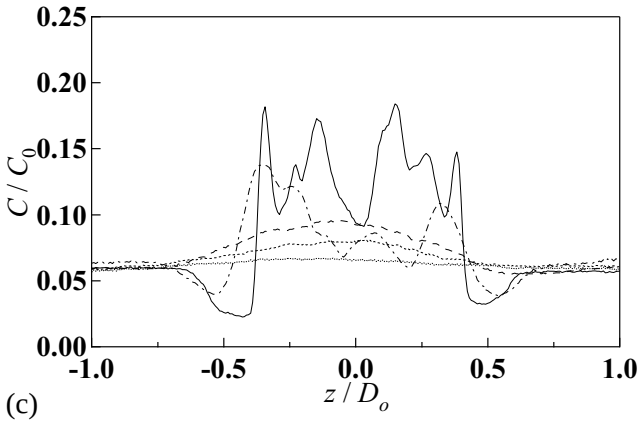

(c)

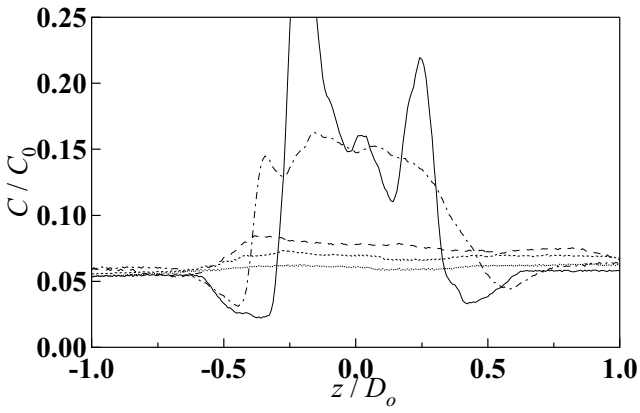

Figure 9 Mean concentration profile; (a)Natural jet, (b)Coaxial Mode (6Hz), (c)Alternative Mode (3Hz, bifurcating plane).

distributions of the mean concentration C normalized with C_0, which is the mean concentration in the initial jet. In the natural jet, C exhibits a top-hat profile at x/D_o <1. At x/D_o >2, C is markedly decreased due to the pinching-off mechanism mentioned above. The peak value is $0.21C_0$ at $x/D_o = 2$. For the controlled jets, C at x/D_o <2 levels off. Note that the vertical axis of Figs. 9 (b) and (c) is enlarged four times that of Fig. 9 (a). At $x/D_o = 2$, the peak value is $0.095C_0$ and $0.081C_0$ for Coaxial and Alternative Modes, respectively. Therefore, it is again confirmed that marked mixing enhancement is achieved with the present control scheme.

4. CONCLUSIONS

A novel coaxial jet nozzle equipped with a row of miniature electromagnetic flap actuators on its outer lip of the annular nozzle is developed. The spatio-temporal flow structures of the controlled jet discharging into an expanded circular duct are studied through flow visualization and quantitative measurements. The following conclusions can be derived:

1) The shedding of large scale vortical structures in the outer shear layer is synchronized with the flap motion, and their magnitude are significantly strengthened.
2) Unsteady recirculation bubble is generated close to the nozzle exit.
3) The mixing between the inner and outer jets are markedly increased through the enhancement of the pinching-off mechanism.
4) Alternative Mode with a subharmonic flapping frequency gives the most effective mixing among various control modes examined.

ACKNOWLEDGMENTS

This work is the results of “Micro Gas Turbine / Fuel Cell Hybrid-Type Distributed Energy System” which is supported by Department of Core Research for Evolutional Science and Technology (CREST) in the program of Japan Science and Technology Corporation (JST). Financial support by Ministry of Education, Science, Culture and Sports through the Grant-in-Aid for Scientific Research (No. 10355010) is also acknowledged.

REFERENCES

[1] Mankbadi, R., Dynamics and Control of Coherent Structure in Turbulent Jets, Appl. Mech. Rev., 45, (1992), pp. 219-248.
[2] Moin, P., and Bewley, T., Feedback Control of Turbulence, Appl. Mech. Rev., 47, (1994), S3-S13.
[3] Kasagi, N., Progress in Direct Numerical Simulation of Turbulent Transport and Its Control, Int. J. Heat & Fluid Flow, 19, (1998), pp. 128-134.
[4] Crow S. C., and Champagne, F. H., Orderly Structure in Jet Turbulence, J. Fluid Mech., 48, (1971), pp. 547-591.
[5] Cantwell, B. J., Organized Motion in Turbulent Flow, Annu. Rev. Fluid Mech., 13, (1981), pp. 437-515.
[6] Robinson, S. K., Coherent Motions in the Turbulent Boundary Layer, Annu. Rev. Fluid Mech., 23, (1991), pp. 601-639.
[7] Ho, C. M., and Tai, Y. C., Review: MEMS and Its Applications for Flow Control, ASME J. Fluids Eng. 118, (1996), pp. 437-447.
[8] McMichael, J. M., Progress and Prospects for Active Flow Control Using Microfabricated Electromechanical Systems (MEMS), AIAA Paper, 96-0306 (1996).
[9] Liu, C., Tsao, T., and Tai, Y. C., Out-of-plane Permalloy Magnetic Actuators for Delta-wing Control," Proc. 8th IEEE MEMS Workshop, Amsterdam, (1995), pp. 7-12.
[10] Smith, B. L., and Glezer, A., "Vectoring and Small Scale Motions Effected in Free Shear Flows Using Synthetic Jet Actuators, AIAA-paper, 97-0213, (1997).
[11] Huang, C., Najafi, K., Alnajjar, E., Christophorou, C., Naguib, A., and Nagib, H. M., Operation Testing of Electrostatic Microactuators and Micromachined Sound Detectors for Active Control of High Speed Flows, Proc. 11th IEEE MEMS Workshop, Heidelburg, (1998), pp. 71-86.
[12] Suzuki, H., Kasagi, N., and Suzuki, Y., Active Control of an Axisymmetric Jet with an Intelligent Nozzle, 1st Int. Symp. Turbulence & Shear Flow Phenomena, Santa Barbara, (1999), pp. 665-670; also submitted to Phys. Fluids, (2000).
[13] Au, H., and Ko, N. W. M., Coaxial Jets of Different Mean Velocity Ratios, J. Sound and Vib., 116, (1987), pp. 427-443.
[14] Rehab, H., Villermaux, E., and Hopfinger, E. J., Flow Regimes of Large-velocity-ratio Coaxial Jets, J. Fluid Mech., 345, (1997), pp. 357-381.